

## Submitted version

Title: Numerical investigation of chatter suppression in milling using active fixtures in open-loop control

Author: L. Sallese, N. Grossi, A. Scippa, G. Campatelli

DOI: <http://dx.doi.org/10.1177/1077546316668686>

Journal: *JOURNAL OF VIBRATION AND CONTROL*

Please cite this article as:

L. Sallese, N. Grossi, A. Scippa, G. Campatelli, Numerical investigation of chatter suppression in milling using active fixtures in open-loop control, *Journal of Vibration and Control*, 24 (2018) 1757-1773, <http://dx.doi.org/10.1177/1077546316668686>

This is a PDF file of a submitted version of an unedited manuscript.

# Numerical investigation of chatter suppression in milling using active fixtures in open-loop control

Lorenzo Sallese<sup>a</sup>, Niccolò Grossi<sup>a\*</sup>, Antonio Scippa<sup>a</sup>, Gianni Campatelli<sup>a</sup>

<sup>a</sup>Department of Industrial Engineering, University of Firenze, Via di Santa Marta 3, 50139, Firenze, Italy

\* Corresponding author. Tel.: +39-055-2758726; fax: +39-055-2758755. E-mail address:

[niccolo.grossi@unifi.it](mailto:niccolo.grossi@unifi.it)

## Abstract

Among the chatter suppression techniques in milling, active fixtures seem to be the most industrially oriented, mainly because these devices could be directly retrofittable to a variety of machine-tools. The actual performances strongly depend on fixture design and the employed control logic. The usual approach in literature, derived from general active vibration control applications, is based on the employment of adaptive closed-loop controls aimed at mitigating the amplitude of chatter frequencies with targeted counteracting vibrations. Whilst this approach has proven its effectiveness, a general application would demand for a wide actuation bandwidth that is practically impeded by inertial forces and actuator related issues. This paper presents the study of the performance of alternative open-loop actuation strategies in suppressing chatter phenomenon, aiming at limiting the required actuation bandwidth. A dedicated time-domain simulation model, integrating fixture dynamics and the features of piezo-electric actuators, is developed and experimentally validated in order to be used as a testing environment to assess the effectiveness of the proposed actuation strategies. An extensive numerical investigation is then carried out to highlight the most influencing factors in assessing the capability of suppressing chatter vibrations. The

results clearly demonstrated that the regenerative effect could be effectively disrupted by actuation frequencies close to half the tooth-pass frequency, as long as adequate displacement is provided by the actuators. This could sensibly increase the critical axial depth of cut and hence improve the achievable material removal rate, as discussed in the paper.

**Keywords:** Active fixtures; milling; chatter; model; control

## **Introduction**

Chatter vibrations in machining processes have collected the focus of several researchers in the last decades, due to their effect in limiting productivity and generating additional issues, such as degrading surface finishing, increasing tool wear and even potentially damaging the machine tool itself (Quintana and Ciurana, 2011). Literature presents various approaches aimed at predicting and preventing the onset of such vibrational instability by means of dedicated experimental tests (Grossi, Scippa, et al., 2015) or analytical models (Altintas and Weck, 2004). Chatter prediction approaches are nowadays extensively adopted in the research field, nevertheless industrial application is still limited by the required expertise in modal analysis (Montevecchi et al., 2015) and time consuming experimental tests. This aspects fostered the study and development of alternative in-process strategies aimed at monitoring the cutting process in real time and intervene on the process itself to mitigate or suppress chatter vibrations (Quintana and Ciurana, 2011). These active approaches have shown the highest flexibility due to the intrinsic capability of intelligently adapting the required counteracting actions in real time by means of active materials and dedicated control logics. Different solutions have been presented and investigated, as discussed in literature (Rashid and Mihai Nicolescu, 2006). Among the different active vibration control (AVC) approaches and devices presented in literature, one of the most industrially

oriented alternative is represented by active fixture, often referred to as active workpiece holder (Abele et al., 2008), (Brecher et al., 2010) , (Ford et al., 2013), given that these devices can generally be retrofittable to different machining tables, without requiring tuning or modifications. Active fixtures are mechatronics systems integrating sensors and actuators with the purpose of monitoring workpiece vibrations during the process and actuate specific counteracting action once chatter is detected. As discussed in previous works (Ganguli et al., 2006), (Weremczuk et al., 2015), modeling and simulating the cutting process, including active fixture behavior, represents a fundamental task in developing effective control strategies to be implemented in the physical active fixtures. Modeling of piezo actuators embedded in the fixture appears to be crucial in order to simulate fixture behavior in a way that is consistent with the real application. For the purpose of modeling the interaction between the active fixture and the cutting process, authors developed a simplified time-domain model, including piezo actuators features, that is presented in this paper, along with the experimental validation tests.

The main goal of developing such a numerical simulative environment was to be used as a testing platform for the investigation of alternative control strategies to mitigate chatter phenomenon. Literature generally describes the development and implementation of alternative closed-loop control strategies aimed counteracting chatter onset by applying counter-vibrations in the proximity of chatter frequency (Abele et al., 2008), (Brecher et al., 2010). Nevertheless, the bandwidths of the investigated systems and chatter vibrations are always limited below 400Hz, that could be not representative of general applications in which chatter frequency can easily exceed the kHz frequency range. Implement such approaches in these cases would demand for sensibly wider bandwidth of the active fixture, but it could generally be impeded by limitations in terms of inertial forces and operability of the actuators. Taking those factors into account authors decided to investigate the effect of different open-loop actuation strategies, constrained within

active fixture exploitable frequency bandwidth, in mitigating the chatter instability. The effects of different actuation parameters have been simulated and are here discussed in order to highlight the most influencing factors in assessing the feasibility and effectiveness of low-frequency actuation strategies in suppressing or mitigating chatter instability.

### **Simplified model of the active fixture**

The design of a control system integrating actuators and sensors requires an accurate knowledge of the transfer functions between the inputs and the outputs of the system. In this paper a simplified model of the system is proposed. The simplest design of an active fixture for milling applications is represented by a two degrees of freedom (DOFs) compliant mechanism based on serial kinematic and incorporating monolithic flexure hinges, as exemplified in previous related works (Ford et al., 2013). The inner stage is generally used to secure the workpiece, while the outer frame is fixed to the machine tool table. By lumping stiffness and damping of the stages (i.e., actuators, flexure hinges, preload springs, etc.), this architecture can be schematized as in Fig. 1, where  $F_{px}$  and  $F_{py}$  represent the force generated along the two DOFs by the actuators, generally piezoelectric ones (Park et al., 2007).

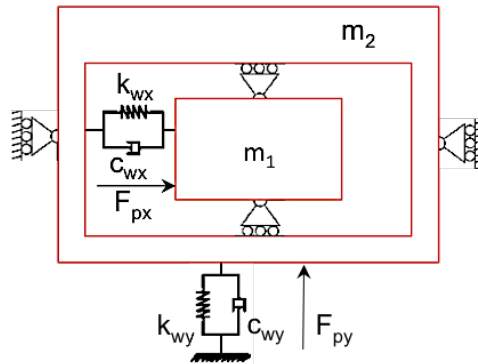


Fig. 1 Basic architecture of an active fixture with two DOFs.

The piezoelectric actuators achieve the purpose of controlling stage displacement by using the inverse piezoelectric properties of piezoelectric materials, which generate shape change if an electric field is applied. The general approach in modelling these effect is by inducing additional workpiece displacement (Weremczuk et al., 2015) in order to simulate the actuation effect, but this simulated effect could often be not consistent with the electrical and physical operability of piezo actuators. Taking those factors into account authors integrated a dedicated model for piezo actuators embedded in the fixture, in order to directly relate the effect of actuators input voltage on fixture behavior.

There are different ways of modelling the inverse piezoelectric effect in order to describe the behavior of piezo actuators, possibly including some level and type of non-linearity, such as hysteresis and creep, that could get relevant in high resolution positioning devices. Nevertheless, according to literature (Adriaens et al., 2000) a linear model that simply relates actuation force to input voltage could be consistent with the specific application. The following relations can be used to define the characteristics of the piezoelectric actuators:

$$[M]\{\ddot{u}\} + [C]\{\dot{u}\} + [K_{uu}]\{u\} + [K_{u\psi}]\{\psi\} = \{f\} \quad (1)$$

$$[K_{u\psi}]^T \{u\} + [K_{\psi\psi}]\{\psi\} = \{q\} \quad (2)$$

where:  $[K_{uu}]$ ,  $[C]$  and  $[M]$  are respectively the mechanical stiffness, damping and mass matrices,  $[K_{\psi\psi}]$  is the dielectric stiffness matrix,  $[K_{u\psi}]$  is the piezoelectric coupling matrix,  $\{u\}$  is the nodal displacement vector,  $\{f\}$  is the vector of the external mechanical forces,  $\{q\}$  and  $\{\psi\}$  are the nodal vectors of the electric charge and scalar electric potential respectively.

### Milling dynamics model

In literature the dynamics of the milling process, considering the regenerative effect, can be described by an n-dimensional linear time periodic system with a single discrete time delay (Altintas, 2012).

Without loss of generality, the simplest analytical description of the milling process involving an active workpiece holder driven by piezo actuators, requires a four DOFs lumped parameters dynamics model as shown in Fig. 2. Actually the milling cutter and the proposed workpiece holder architecture can be considered to have two orthogonal DOFs both. In this work the cutter is assumed to have N number of teeth with a zero helix angle in order to reduce computational effort, due to the needed z-level discretization of the helix angle.

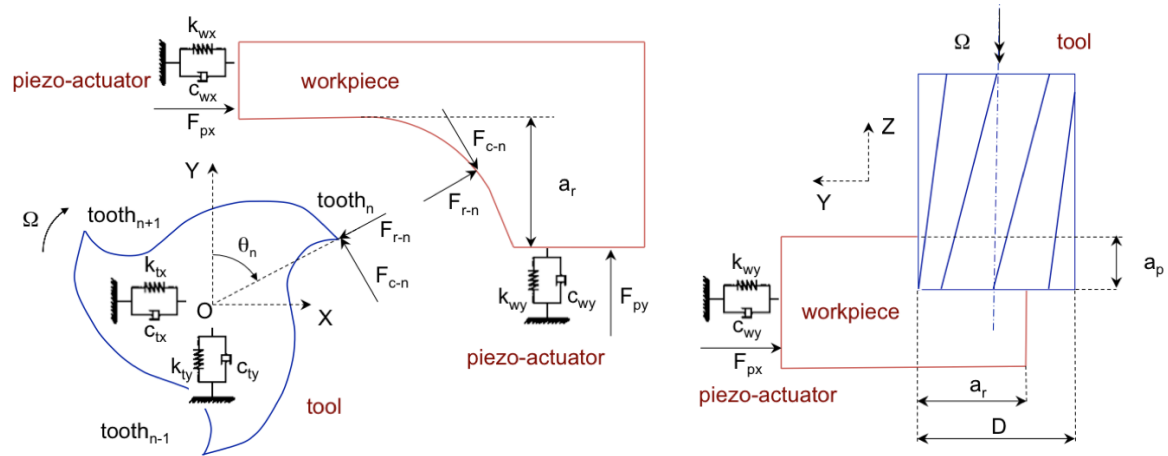


Fig. 2 Dynamic end milling system with active workpiece holder.

The governing equation of the milling process shown in Fig. 2 can be formulated as the following differential equation systems:

$$\begin{cases}
 \ddot{x}_t(t) + 2\zeta_{t_x}\omega_{t_x}\dot{x}_t(t) + \omega_{t_x}^2x_t(t) = \frac{\omega_{t_x}^2}{k_{t_x}} \cdot F_x(t) \\
 \ddot{y}_t(t) + 2\zeta_{t_y}\omega_{t_y}\dot{y}_t(t) + \omega_{t_y}^2y_t(t) = \frac{\omega_{t_y}^2}{k_{t_y}} \cdot F_y(t) \\
 \ddot{x}_w(t) + 2\zeta_{w_x}\omega_{w_x}\dot{x}_w(t) + \omega_{w_x}^2x_w(t) = -\frac{\omega_{w_x}^2}{k_{w_x}} \cdot [F_x(t) + k_{\psi_x}\psi_x(t)] \\
 \ddot{y}_w(t) + 2\zeta_{w_y}\omega_{w_y}\dot{y}_w(t) + \omega_{w_y}^2y_w(t) = -\frac{\omega_{w_y}^2}{k_{w_y}} \cdot [F_y(t) + k_{\psi_y}\psi_y(t)]
 \end{cases} \quad (3)$$

where the subscripts  $t$  and  $w$  identify respectively the tool and the workpiece,  $\zeta$  is the damping coefficient,  $\omega$  is the angular natural frequency, and  $k$  is the modal stiffness, while  $\psi_x$  and  $\psi_y$  are the instantaneous electric potential applied to the controlled piezo actuator along the X and Y direction respectively.

The forces  $F_x(t)$  and  $F_y(t)$  excite tool and workpiece in the feed (X) and normal (Y) directions, causing dynamic displacements  $\Delta x(t)$  and  $\Delta y(t)$  respectively, which are responsible of the



regenerative instability:

$$\Delta x(t) = (x_t(t) - x_w(t)) - (x_t(t-T) - x_w(t-T)) \quad (4)$$

$$\Delta y(t) = (y_t(t) - y_w(t)) - (y_t(t-T) - y_w(t-T)) \quad (5)$$

where T is the tooth passing interval.

According to mechanistic cutting force model (Altintas and Weck, 2004) the tangential and normal cutting force components for the  $k$ th tooth,  $F_{ck}$  and  $F_{rk}$ , can be related to the axial depth of cut  $a_p$  and the instantaneous chip thickness  $h_k(t)$  using constant cutting coefficients  $K_{tc}$ ,  $K_{te}$ ,  $K_{rc}$ , and  $K_{re}$ .

$$F_{ck}(t) = K_{tc} a_p h_k(t) + K_{te} a_p \quad (6)$$

$$F_{rk}(t) = K_{rc} a_p h_k(t) + K_{re} a_p \quad (7)$$

The regenerative instantaneous chip thickness  $h_k(t)$  can be assumed to be the sum of the kinematic chip thickness and the regenerative dynamic chip thickness, which is related to the dynamic displacements  $\Delta x(t)$  and  $\Delta y(t)$  projected in the chip thickness direction:

$$h_k(t) = [(f_z + \Delta x(t)) \cdot \sin(\phi_k(t)) + \Delta y(t) \cdot \cos(\phi_k(t))] \cdot g(\phi_k(t)) \quad (8)$$

where the function  $g(\phi_k(t))$ , is used to indicate the engagement of the tooth:

$$g(\phi_k(t)) = \begin{cases} 1 & \text{if } \phi_{st} < \phi_k(t) < \phi_{ex} \\ 0 & \text{otherwise} \end{cases} \quad (9)$$

in which  $\phi_{st}$  and  $\phi_{ex}$  are respectively the start and exit immersion angles of the cutter. For up-milling  $\phi_{st} = 0$  and  $\phi_{ex} = \arccos(1 - 2a_r/D)$ , while for down-milling  $\phi_{st} = \arccos(2a_r/D - 1)$ , and  $\phi_{ex} = \pi$ , being  $a_r/D$  the radial immersion ratio (radial depth of cut / tool diameter).

Resolving the cutting forces in the X and Y directions leads to:

$$F_x = -\sum_{k=0}^{N-1} F_{ck}(t) \cdot \cos(\phi_k(t)) + F_{rk}(t) \cdot \sin(\phi_k(t)) \quad (10)$$

$$F_y = \sum_{k=0}^{N-1} F_{ck}(t) \cdot \sin(\phi_k(t)) - F_{rk}(t) \cdot \cos(\phi_k(t)) \quad (11)$$

By rearranging the previous equations, it is possible to reduce the dynamics of the milling process, Eq. 3 to an equivalent coupled delayed differential equation (DDE):

$$\begin{aligned} \mathbf{M} \cdot \ddot{\mathbf{X}}(t) + \mathbf{C} \cdot \dot{\mathbf{X}}_n(t) + \mathbf{K} \cdot \mathbf{X}(t) = \\ = \mathbf{K}_c(t)(\mathbf{X}(t) - \mathbf{X}(t-T)) + \mathbf{K}_\psi \psi \end{aligned} \quad (12)$$

where  $\mathbf{M}$ ,  $\mathbf{C}$ ,  $\mathbf{K}$  and  $\mathbf{X}(t)$  represent the mass matrix, damping matrix, stiffness matrix and displacement vector of the system (4 DOFs), respectively, while  $\mathbf{K}_c(t)$  is the cutting force coefficient matrix,  $\mathbf{K}_\psi$  is the dielectric stiffness matrix and  $\{\psi\}$  is the nodal vector of scalar electric potential.

### Time domain numerical approach

The dynamic milling process considering the regenerative effect is generally modeled as a linear time periodic system with a single discrete time delay, which can be approximately solved by using the analytical or numerical methods (Altintas, 2012), (Kyrychko and Hogan, 2010).

Time domain numerical simulation methods are quite powerful: they are capable of taking into account true kinematics of the milling process, mechanics of cutting, the influence of inner and outer modulation, cutter geometry, run-out and other non-linearities, but their computational cost is normally too high.

In this paper a full-discretization method based on an implicit direct integration scheme is proposed. It was selected due to its high computational efficiency and second order accuracy.

The first step to solve Eq. 12 numerically is to discretize the time period  $T$ , hence equally divide  $T$  into  $m$  small time intervals,  $T = m \cdot \Delta t$ , where  $m$  is an integer. For each time interval  $t_n = t_0 + n \cdot \Delta t$  the response  $X_n = X(t_n)$  of Eq. 12 with the initial condition  $X_0 = X(t_0)$ ,  $\dot{X}_0 = \dot{X}(t_0)$ ,  $\ddot{X}_0 = \ddot{X}(t_0)$  can be obtained via the direct Newmark integration scheme (Newmark, 1959). The Newmark method relies on the following interpolations that relate positions  $X(t)$ , velocities  $\dot{X}(t)$ , and accelerations  $\ddot{X}(t)$ , from step  $n$  to step  $n + 1$ :

$$X_{n+1} = X_n + \Delta t \cdot \dot{X}_n + \frac{\Delta t^2}{2} \cdot [(1 - 2\beta) \cdot \ddot{X}_n + 2\beta \cdot \ddot{X}_{n+1}] \quad (13)$$

$$\dot{X}_{n+1} = \dot{X}_n + \Delta t \cdot [(1 - \gamma) \cdot \ddot{X}_n + \gamma \cdot \ddot{X}_{n+1}] \quad (14)$$

where  $X_n$ ,  $\dot{X}_n$ ,  $\ddot{X}_n$  are approximations to the position, velocity, and acceleration vectors at time step  $n$ ,  $\Delta t$  is the time step size, and  $\beta$  and  $\gamma$  are the free parameters of integration.

For  $\gamma = 1/2$  and  $\beta = 1/4$  the method is reduced to the trapezoidal rule and is energy conserving (Bathe and Saunders, 1984). This choice of parameters leads to averaging acceleration in  $[t_n, t_{n+1}]$ . If  $\gamma > 1/2$  and  $\beta > 1/4 \cdot (1/2 + \gamma)^2$  numerical damping is induced into the solution leading to a loss of energy and momentum. In this work the average constant acceleration scheme (i.e.,  $\gamma = 1/2$  and  $\beta = 1/4$ ) has been considered, as it represents the unconditionally stable scheme (i.e., implicit), with asymptotically the highest accuracy (Bathe and Saunders, 1984), (Hughes, 2000).

The interpolations of Eq. 13 and Eq. 14 can be directly introduced into the equations of motions (i.e., Eq. 12). This leads to a set of algebraic equations that can be either linear or non-linear, depending on the type of problem, with  $\ddot{X}_{n+1}$  as the resulting unknowns. A set of linear equations is obtained if a linear cutting force model is used, as that proposed in this work.

Application of the Newmark method to the direct time-integration of Eq. 12 requires a three-step procedure:

1. Evaluation of the system displacements and velocities at the time step n+1 (predictor phase):

$$\tilde{X}_{n+1} = X_n + \Delta t \cdot \dot{X}_n + \frac{\Delta t^2}{2} \cdot (1 - 2\beta) \cdot \ddot{X}_n \quad (15)$$

$$\tilde{\dot{X}}_{n+1} = \dot{X}_n + \Delta t \cdot (1 - \gamma) \cdot \ddot{X}_n \quad (16)$$

2. Resolution of the above system of equations, resulting from the substitution of Eq. 13 and Eq. 14 into Eq. 12, for  $\ddot{X}_{n+1}$ :

$$\begin{aligned} [\mathbf{M} + \mathbf{C} \cdot \gamma \cdot \Delta t + (\mathbf{K} - \mathbf{K}_c) \cdot \beta \cdot \Delta t^2] \cdot \ddot{X}_{n+1} = \\ \mathbf{K}_y \psi_{n+1} - \mathbf{K}_c X_{n+1-m} - \mathbf{C} \cdot \tilde{\dot{X}}_n - (\mathbf{K} - \mathbf{K}_c) \cdot \tilde{X}_n \end{aligned} \quad (17)$$

If the time-step  $\Delta t$  is uniform, the system matrix of Eq. 17 can be factored once.

3. Substitution of the result into expression to obtain  $X_{n+1}$  and  $\dot{X}_{n+1}$  (corrector phase).

$$X_{n+1} = \tilde{X}_{n+1} + \beta \cdot \Delta t^2 \cdot \ddot{X}_{n+1} \quad (18)$$

$$\dot{X}_{n+1} = \tilde{\dot{X}}_{n+1} + \gamma \cdot \Delta t \cdot \ddot{X}_{n+1} \quad (19)$$

This implementation is very efficient, and may be also carried out for nonlinear problems, by customarily solving the resulting set of nonlinear algebraic equations in  $\ddot{X}_{n+1}$  with either Newton-Raphson iteration, which has a quadratic convergence in the proximity of the solution, secant methods, or quasi-Newton method (Hughes, 2000).

### Experimental validation

To prove the accuracy of the proposed approach, an experimental validation was carried out using a Mori Seiki NMV1500 DCG 5-axis vertical milling machine. Selected test workpiece was a

block of 6082-T4 aluminum, fixed on a Kistler 9257A piezoelectric dynamometer, as shown in Fig. 3a.

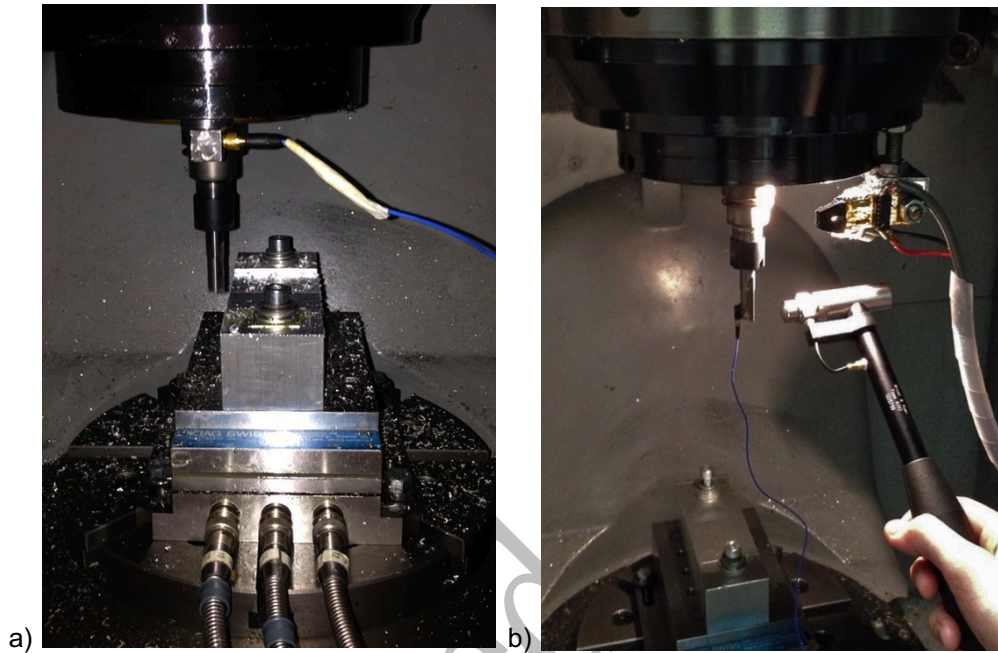


Fig. 3 a) Cutting tests setup, b) Tooling impact testing.

Several cutting tests in slotting operations were performed at different depths of cut. A 10 mm Garant 201320 end mill, with regular pitch and null helix angle was used in order to avoid the influence of the helix angle on cutting forces. The cutting speed was set to 140 m/min (4458 rpm) according to the suggested tool parameters.

Tooltip Frequency Response Function (FRF) was measured with LMS SCADAS III acquisition system, using a Brüel&Kjær 8202 instrumented hammer and a PCB 352C22 accelerometer (0.5g), as shown in Fig. 3b.

Modal curve-fitting allowed identifying modal parameters of an equivalent single degree of freedom system, for both tooling and fixture (i.e., piezoelectric dynamometer), as exemplified in Fig. 4 for the tooling FRFs.

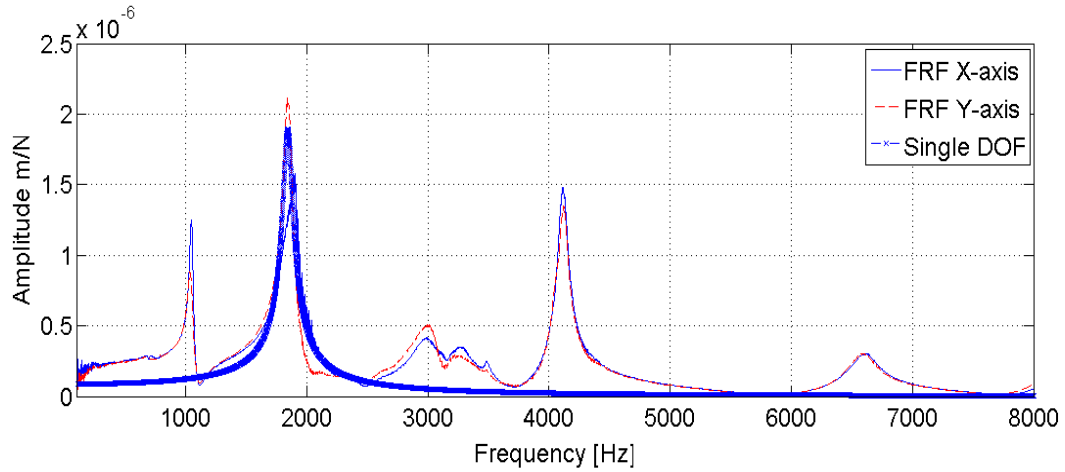


Fig. 4 Experimental tooltip FRFs and curve fitted single degree of freedom FRF.

Table 1 summarizes the identified modal parameters for tooling and fixture along X-axis, tooling and fixture dynamics was approximately equal in X and Y directions:

Table 1 Identified modal parameters.

	Natural frequency, $f_n$	Damping coefficient, $\zeta$	Modal stiffness, $k$
Tooling	1836 Hz	0.0231	$1.15e^7$ N/m
Fixture	2120 Hz	0.0231	$1.05e^9$ N/m

Cutting force coefficients were estimated on the average measured cutting forces in stable slotting operations at different feed per tooth ( $f_z$ ), close to the recommended value (i.e.,  $f_z = 0.05$  mm/rev per tooth), as discussed by authors in a previous work (Grossi, Sallese, et al., 2015). The identified coefficients are reported in Table 2.

Tool run-out was experimentally measured: 20  $\mu$ m.

Table 2 Identified cutting force coefficients.

$K_{tc}$ (N/mm <sup>2</sup> )	$K_{te}$ (N/mm)	$K_{rc}$ (N/mm <sup>2</sup> )	$K_{re}$ (N/mm)
1086.66	764.29	139.03	33.32

Fig. 5 shows a comparison of experimental and estimated cutting forces ( $A_p=0.8\text{mm}$ ) in which the simulation has been performed considering a tool with a single tooth, and the feed per tooth increased of the measured run-out ( $f_z = 0.09\text{ mm}$ ), because the model neglects tool run-out currently. The measured cutting forces were dynamically compensated in order to ensure adequate accuracy (Scippa et al., 2015).

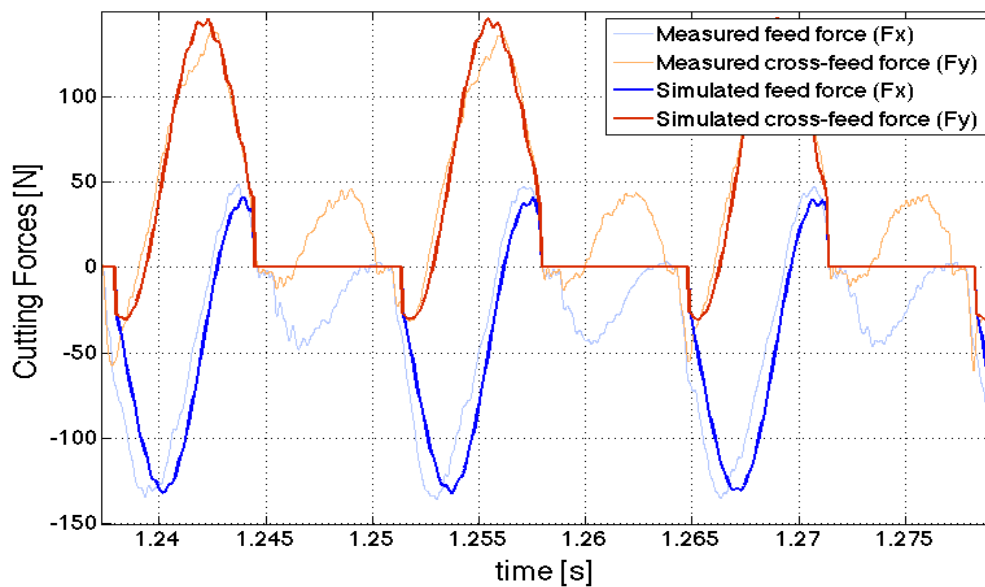


Fig. 5 Measured and simulated cutting forces.

The predicted and measured cutting forces are in good agreement, which indicates the accuracy of the proposed time domain model. Analogous results were obtained for all the validation tests.

The model is capable of correctly simulating stable and unstable cutting conditions as well as the onset of chatter phenomenon. By increasing axial depth of cut to  $A_p=1\text{mm}$ , cutting forces clearly show the growth of chatter vibrations and the development of a new “pseudo-stable” cutting condition. This is consistent with the periodic disengagement of the tool, which is the main cause of chatter marks on the workpiece and associated with chatter vibrations. This aspect is described by the simulated cutting force time-series reported in Fig. 6, in which the transition phase and the “pseudo-stable” condition are highlighted.

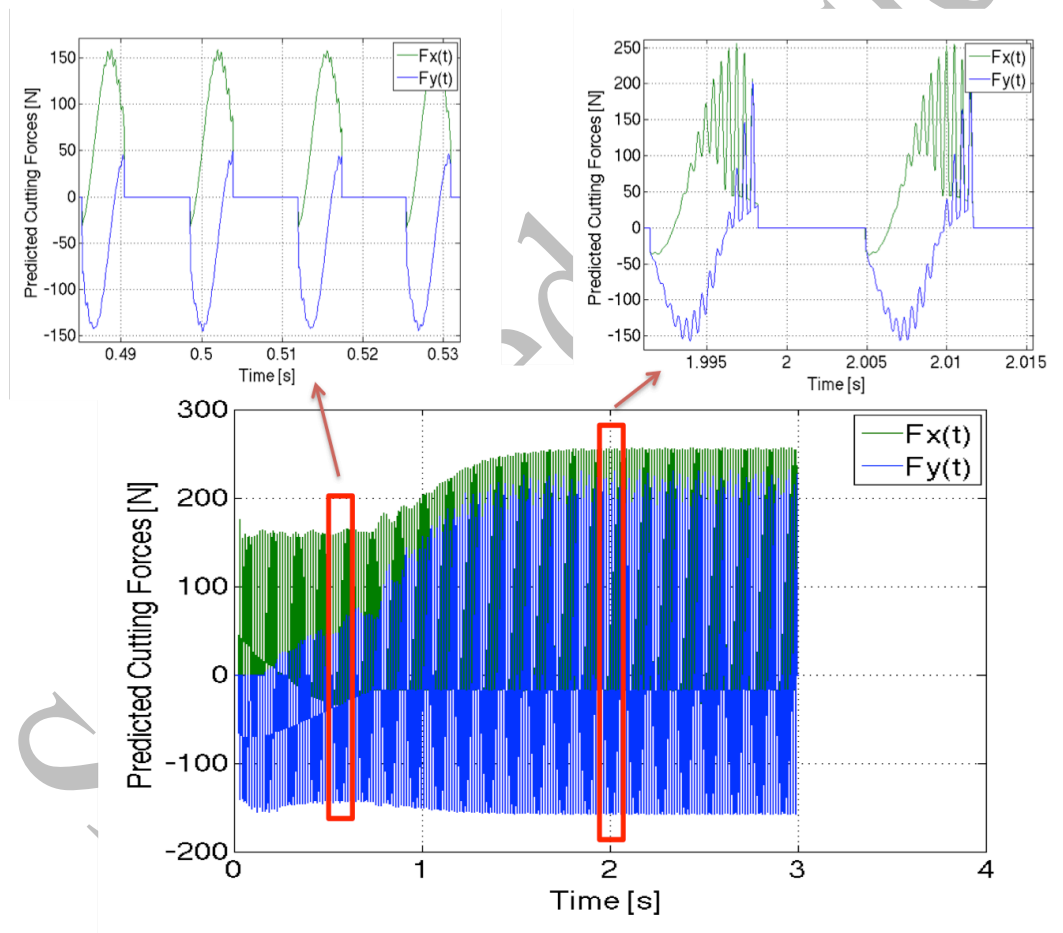


Fig. 6 Analysis of predicted cutting forces in case of chatter.



The proposed time domain model has been implemented in a Matlab ® code. The simulation of a 3 s slotting tests takes about 13 s on a 1.7 Ghz Intel dual core I7 processor with 8 Gb Ram, using a time step of 0.0168 ms (800 time intervals over the period T).

### **Simulation set-up**

Given that the goal was to investigate the effectiveness of different actuation strategies on active fixtures, the features of a real prototype (i.e., fixture dynamics and actuators specifications) have been implemented in the time domain model and realistic cutting conditions have been recreated.

#### *Active fixture design*

The features of the prototype fixture to be implemented in the time domain simulations have been defined based on a prototype fixture designed and developed by authors. The prototype fixture is based on the two DOFs serial kinematics architecture previously described, the 3D model is presented in Fig. 7.

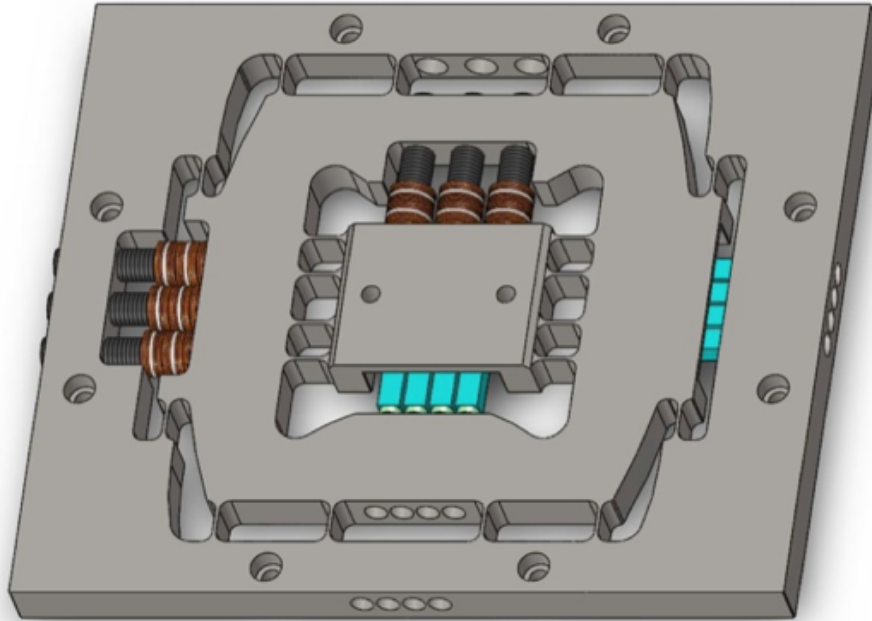


Fig. 7 3D model of the active fixture prototype.

As shown in Fig. 7 the active fixture integrates flexure hinges in order to decouple actuation directions, while maintaining adequate guiding of the motion generated by piezo actuators and ensure the required stiffness. Each axis is driven by four piezoelectric actuators, whose specifications are reported in Table 3. Adequate preload is applied by disc springs acting against the piezo actuators in order to prevent tensile stress on the actuators.

Table 3 Main specifications of the selected piezo actuators.

Blocking force	Max. displacement	Max. voltage	Stiffness
3200 N	32 $\mu\text{m}$	200 V	100 N/ $\mu\text{m}$

The coefficients of the dielectric coupling matrix can easily be derived from the actuators specifications by simply dividing the maximum achievable force (i.e., blocking force) by the maximum operable voltage. For this application, based on the described actuator specifications,

a coefficient  $K_{\psi\psi} = 16 \text{ N/V}$  can be estimated for each single actuators.

In order to identify fixture dynamics along the actuation direction, the frequency response function of each actuation axis, obtained by finite element analysis, have been curve fitted with a single DOF, as for the tooling. The identified parameters are reported in Table 4.

Table 4 active fixture estimated modal parameters.

	Inner stage	Outer stage
Stiffness, $k$	$4.28e^8 \text{ N/m}$	$4.39e^8 \text{ N/m}$
Damping coeff., $\zeta$	0.0432	0.0432
Natural freq., $f_n$	2689.8 Hz	1782.8 Hz

#### *Cutting conditions*

The simulated cutting conditions have been defined in accordance with the experimental validation tests: tooling dynamics was set as identified by modal curve-fitting the tool-tip FRFs and the cutting parameters were set starting from the ones used in the experimental tests (i.e., suggested parameters). Slotting operations were simulated and subsequently different rotational speeds and feed rates were tested in order to extend the investigation, as discussed in the following section.

As described in the experimental validation tests, the dominant frequency of the tooling, responsible for chatter instability, if workpiece dynamics contribution is neglected, is sensibly higher than the ones reported in previous work on active fixtures (Brecher et al., 2010),(Ford et al., 2013), resembling most practical applications. Implementing a closed-loop control strategy targeted in the chatter frequency band would imply actuating at around 2 kHz, exceeding the outer stage natural frequency. In practical applications this would be made impossible by inertial forces and electrical operability of actuators. Taking this aspect into account authors decided to test open-loop actuation strategies aimed at disrupting the periodicity of the regenerative phenomenon that can determine and maintain chatter vibrations, using sine waves excitations

constrained below 300 Hz. This would represent the most easily implementable control in a physical prototype taking into account both physical and computational constraints.

The main parameters defining different actuation strategies could hence be: actuation frequency, amplitude (voltage provided to actuators) and phase.

#### *Proposed evaluation approach*

In order to assess the effectiveness of the investigated actuation strategies effectiveness the reference parameter was the maximum depth of cut ( $A_{p\text{limit}}$ ) achievable in stable condition.  $A_{p\text{limit}}$  was identified performing process simulations, increasing the depth of cut ( $A_p$ ) until reaching unstable cutting conditions. Depth of cut resolution was set to 0.02 mm and chatter was detected on the basis of tool-tip displacement frequency spectrum when a dominant frequency (i.e., chatter frequency) exceeds the amplitude of nominal chatter-free spectrum (i.e., tooth pass frequency and its harmonics), as in (Grossi, Scippa, et al., 2015).

This approach was repeated for several spindle speeds in order to numerically compute the Stability Lobe Diagram (SLD). First of all, nominal SLD (i.e., without actuation) obtained by the proposed model was compared with the analytically predicted one (Altintas and Weck, 2004), often used as reference, in literature and in practical applications. Fig. 8 shows a good agreement between the two diagrams, differences are in line with  $A_p$  resolution. Comparison proves the reliability of the model in predicting stable and unstable conditions and the accuracy of the proposed evaluation approach in identifying the  $A_{p\text{limit}}$ .

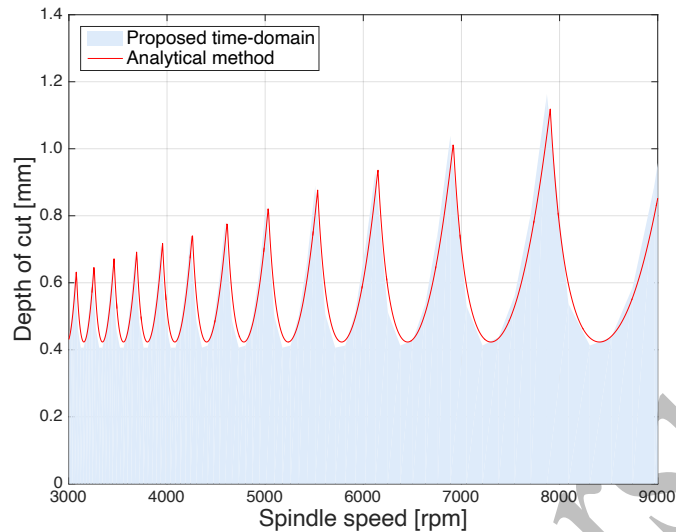


Fig. 8 Validation of SLD obtained via proposed method

## Results

After the assessment of the evaluation approach and the model capability of predicting chatter onset, open-loop actuation strategies were tested. The first investigation was carried out in order to analyse the influence of actuation frequency ( $f_A$ ), that seems the governing parameter: a sine wave signal at different frequencies was provided by actuators, virtually operated at maximum voltage (i.e., 200 V) on both directions, in order to reach a fixed displacement ( $A \approx 0.03$  mm). Fig. 9 shows the effect of sine waves at 187 Hz and 300 Hz within the 3000-7500 rpm spindle speed range of the SLD.

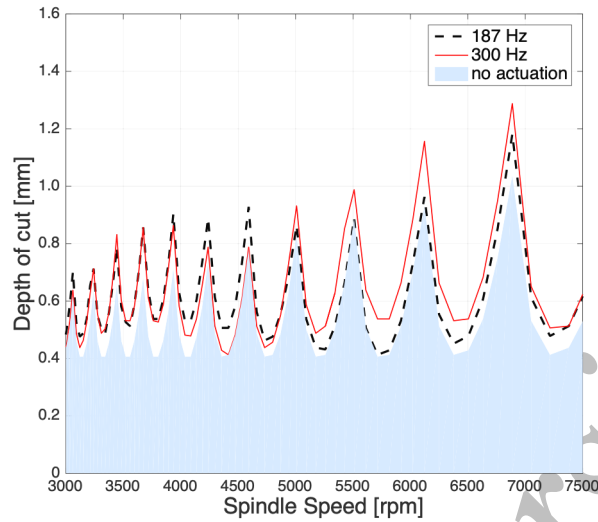


Fig. 9 SLD with open-loop actuation at different frequency

As clearly shown, the maximum depth of cut in stable condition is increased, for most of the spindle speeds. Generating workpiece vibrations at specific frequencies seems hence capable of disrupting the periodicity of the regenerative effect that generates the instability, bringing the system back to stable conditions. This effect extends until a drastic chatter condition is reached (i.e., higher  $A_p$ ). In Fig. 10 the effect of workpiece vibrations on suppressing chatter vibrations is exemplified for a simulated test with 7051 rpm spindle speed and 0.6 mm depth of cut. The actuation (i.e., 300 Hz sine wave) is switched on after 2 s and the instability is damped.

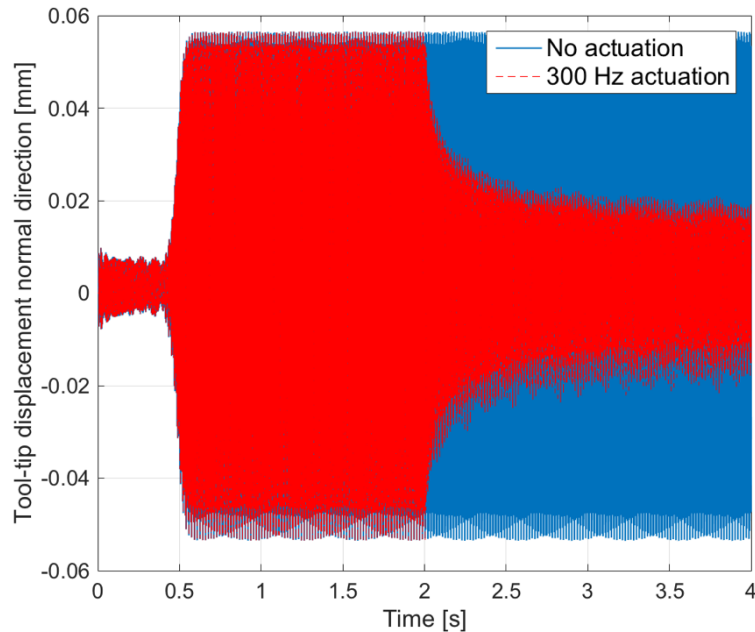


Fig. 10 300 Hz Actuation effect on tool-tip displacement (starting at 2 s, 7051 rpm, 0.6 mm depth of cut)

The described effect on the stability limit is not equal all over the investigated spindle speed range (Fig. 9). The effect of workpiece excitation in extending the stability limits becomes negligible as actuation frequency gets close to the tooth pass frequency ( $f_{tp}$ ) and its harmonics. Taking the 300 Hz actuation tests as an example, the  $A_{p\text{limit}}$  value is not altered in simulated cutting with 4500 rpm ( $f_{tp}=150$  Hz) and 3000 rpm ( $f_{tp}=100$  Hz) spindle speeds, for which 300 Hz represents respectively the second and the third harmonic of the tooth pass frequency. This is consistent with the fact that exciting the workpiece at one of the tooth pass frequency contributions does not influence chatter regenerative effect, because it does not appreciably alter the periodic nature of the process. On the other hand, the effect of the 300 Hz actuation gets significant at different spindle speeds, until generating an increase of about 30% of  $A_{p\text{limit}}$ .

This aspect can be further summarized by aggregating data of different tests with different actuation frequencies and plotting the limit axial depth of cut increase as a function of actuation

frequency ( $f_A$ ) to rotational frequency ( $f_R=n/60$ ) ratio. Fig. 11 shows the results obtained with the aggregated data.

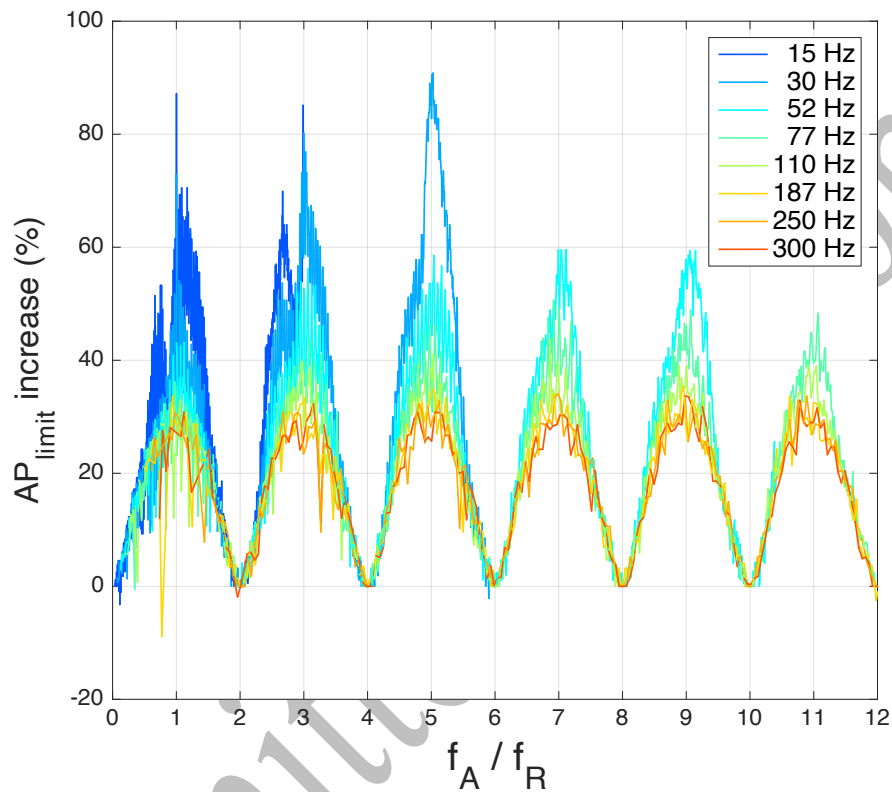


Fig. 11 Actuation frequency effect on rotational frequency

For each actuation frequency tested (i.e., 15÷300 Hz), the minimum  $AP_{limit}$  increase is obtained when actuation frequency matches the tooth pass frequency and its harmonics ( $f_A/f_R = 2, 4, 6, \dots$  for 2 fluted endmill). Moreover, low frequency actuation seems to provide higher improvements.

#### Number of flutes

In order to extend the investigation beyond the results obtained for the 2 fluted endmill, new SLDs were computed simulating tools with different number of flutes and maintaining the 300 Hz actuation frequency, as in most of the examples previously discussed.



The results achieved in these additional tests, in terms of increased stability limits, are summarized with the SLDs reported in Fig. 12a and Fig. 13a for a three and four fluted endmill respectively.

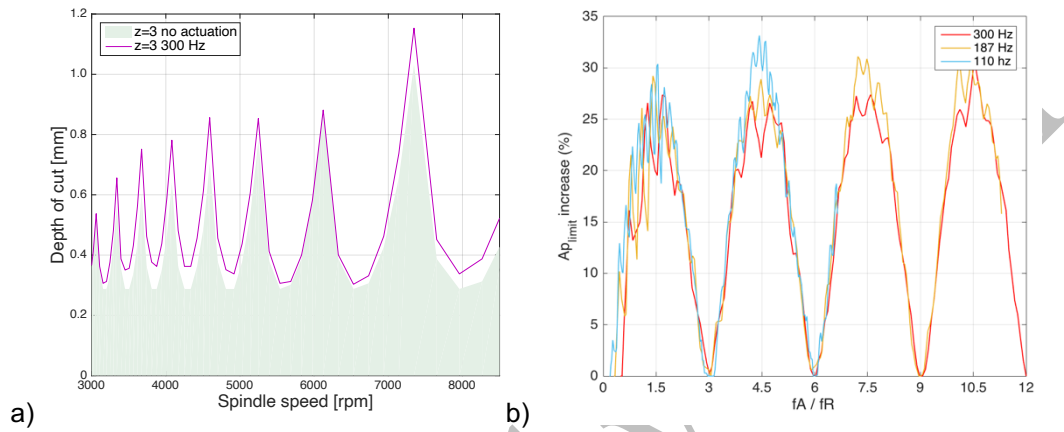


Fig. 12 a) SLD 300 Hz actuation b) Actuation frequency effect on rotational frequency for 3 fluted endmill.

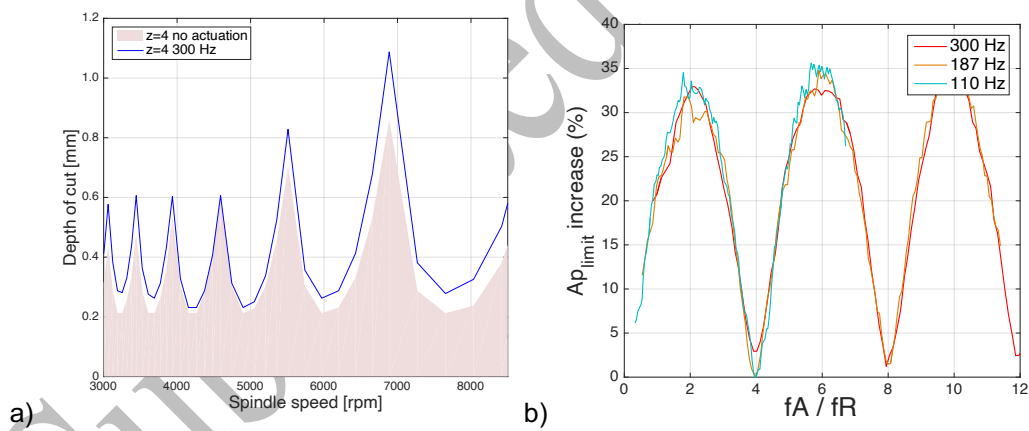


Fig. 13 a) SLD 300 Hz actuation b) Actuation frequency effect on rotational frequency for 4 fluted endmill.

The effect generated by the 300 Hz actuation on the simulations for the three and four flutes is obviously different over the spindle speed range investigated, however the same behaviour at the tooth pass frequency can be observed again. This aspect is confirmed by aggregating results as in Fig. 12b and Fig. 13b where actuation frequency effect is reported one more time as a function

of actuation frequency to rotational frequency ratio.

Results for different number of flutes demonstrated that the effect on chatter stability is minimum on the tooth pass frequency and suggested the optimal actuation frequency equal to:

$$f_A = z \left( k + \frac{1}{2} \right) f_R \quad k = 0, 1, 2, \dots \quad (20)$$

where  $f_A$  is the actuation frequency,  $f_R$  the rotational frequency and  $z$  is the number of flutes.

#### *Actuation direction and phase*

Once that the effect of actuation frequency was highlighted, the focus was put on actuation direction and phase of the excitation sine waves. Simulations showed a negligible influence of actuation signals phase on the stability limit increase. This is consistent with the fact that the proposed open-loop actuation strategy is not focused on counter-acting a specific effect but altering the process periodicity, so it is not strictly dependent on actuation offset, as long as actuation frequency itself allows for periodicity to be interrupted.

On the contrary, actuation direction clearly affects the achievable stable depth of cut, as shown in Fig. 14.

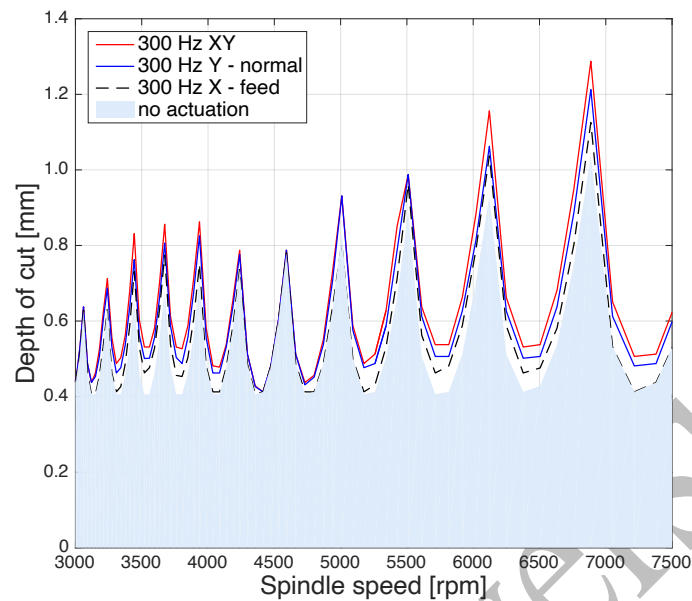


Fig. 14 SLD for different actuation directions

Cross-feed (normal) direction seems to provide better results in increasing the stable depth of cut than actuation on feed direction. This is probably due to cutting forces and tool-tip displacement that are generally higher on normal direction. However, the best results are achieved by actuating on both directions.

#### *Tool dynamics influence*

In order to show the effects of the tooling dynamics on the achievable results, different tooling systems were simulated. In particular tool natural frequency was set to 1000 Hz and 2500 Hz and the related SLDs were computed (Fig. 15), simulating a two fluted mill.

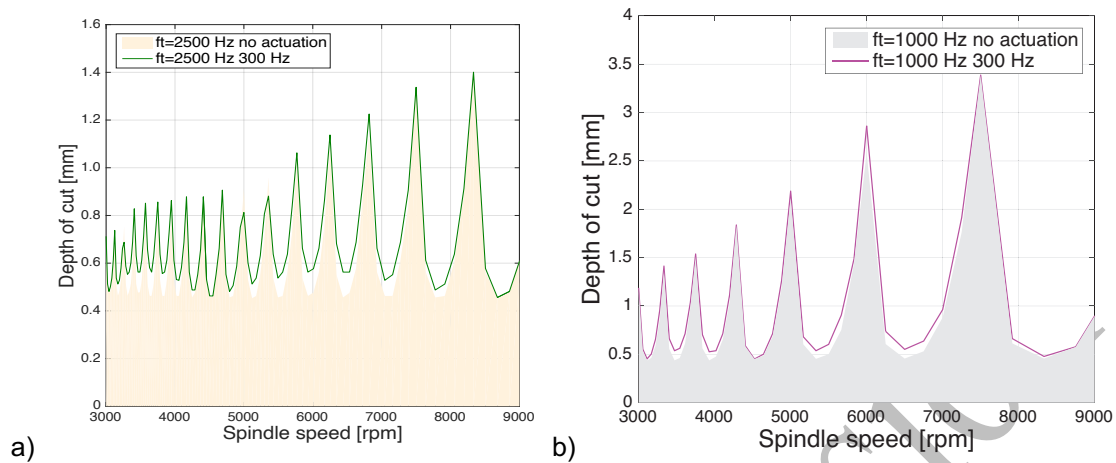


Fig. 15 SLD for a) 2500 Hz b) 1000 Hz tool natural frequency

As reported, the 300 Hz actuation provides appreciable results in both cases and the achievable stability limits (i.e., solid lines in Fig. 15) show the same trend previously discussed. Shall be highlighted, indeed, that the minimum improvement is achieved for the tests with 3000 rpm and 4500 rpm tests, as obtained for the previous tests summarized in Fig. 11, confirming again the dependency on the rotational frequency and suggesting the negligible effect of tooling dynamics (i.e., chatter frequency value).

#### *Actuation amplitude and feed per tooth*

As a final investigation, the effect of feed per tooth ( $f_z$ ) on the achievable stability limits was analysed. The results obtained using 300 Hz actuation in three different test configurations (i.e., different feed per tooth,  $f_z$ ) are presented in Fig. 16.

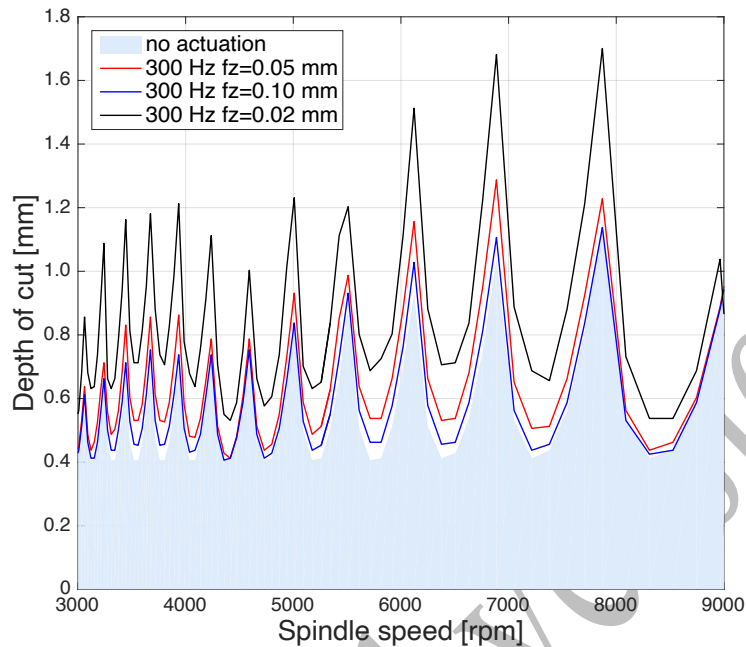


Fig. 16 SLD for different feed per tooth

As shown, by increasing feed per tooth, the actuation effect clearly decreases. Authors assume it to be related to an increase of chip thickness (directly proportional to  $f_z$ ): proposed actuation strategy is indeed disrupting chatter phenomenon by altering chip thickness periodicity. The impact of such a strategy is hence strongly dependent on the relation between chip thickness and actuated workpiece displacement. In order to highlight this dependency, the effect of excited workpiece displacement ( $A$ ) was investigated by keeping a constant  $f_z = 0.05$  mm and computing SLDs using 300 Hz actuation with three different amplitudes (i.e., three displacements magnitudes corresponding to three different input voltages to piezo actuators). Results are shown in Fig. 17.

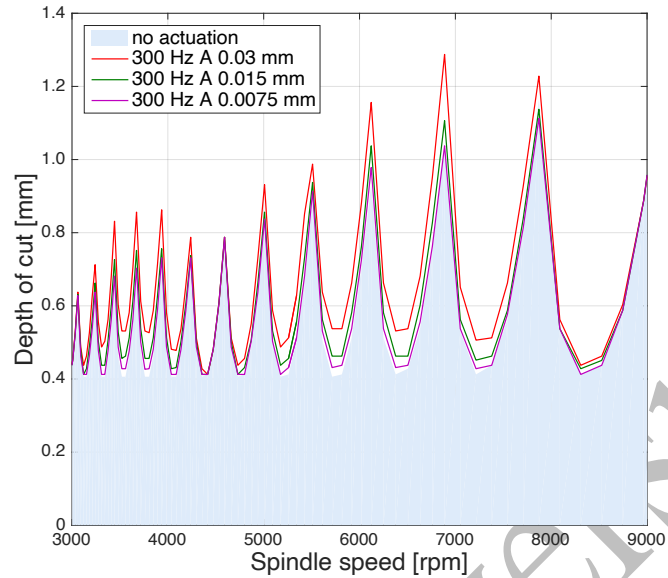


Fig. 17 SLD for different actuated workpiece displacement

Results showed that the higher the actuated workpiece displacement, the higher the stable depth of cut improvement, as expected. In order to further assess the influence of both  $f_z$  and  $A$ , depth of cut increase was identified by simulating tests with a fixed spindle speed ( $n=7051$  rpm) and varying the two parameters individually. Results are shown in Fig. 18a as a matrix in a 3d bar plot.

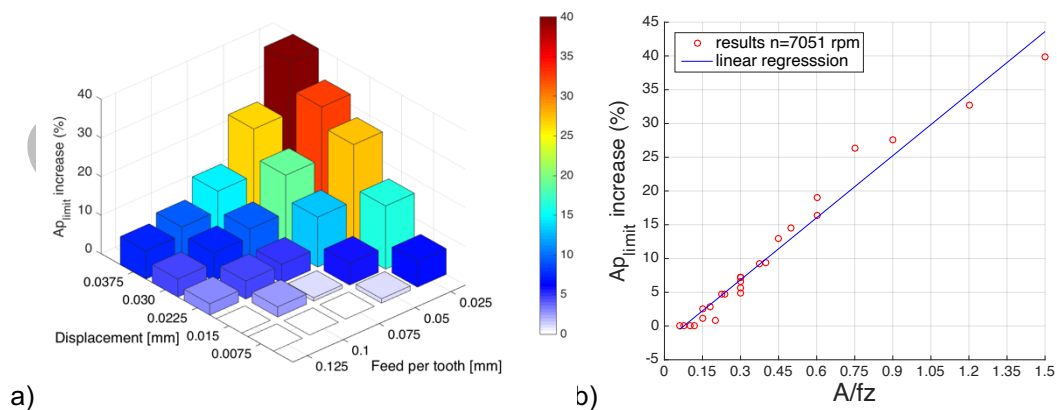


Fig. 18 Depth of cut increase for 7051 rpm, varying actuated displacement and feed per tooth

Fig. 18a shows that the actuation strategy effectiveness is directly proportional to displacement and inversely proportional to feed per tooth. Actually,  $A/f_z$  ratio seems to be one of the key parameter in assessing an effective actuation, as should be expected since a lower  $A/f_z$  ratio is representative of cases in which chip thickness is sensibly higher than the actuated displacement and hence the effect could only be limited. This aspect is confirmed by the fact that the main matrix diagonal reporting tests with the same  $A/f_z$  (equal to 0.3) shows very similar and reduced depth of cut improvement (blue bars).

In order to formalize this aspect, generated results are reported in Fig. 18b, where the dependency between  $A_{p\text{limit}}$  increase and  $A/f_z$  shows a linear behaviour. In addition, the results showed that in order to provide a significant effect on the stable axial depth of cut (i.e., at least a 5% improvement),  $A/f_z$  ratio should exceed 0.25. Thus in order to exploit such an actuation strategy in practical applications, designing fixture frame and selecting actuators in order to reach the required displacement magnitude appears to be crucial.

## Conclusions

This paper presented a time-domain simulation model dedicated to active fixturing in milling applications. Following a common fixture architecture, based on serial kinematics, the fixture dynamics have been defined as a two degrees of freedom lumped model along each actuation directions. Actuation force of the embedded piezo-electric actuators has been modelled defining a linear relation with the provided voltage, as suggested in literature. The model has been experimentally validated with satisfactory results.

The developed model has then been used as a testing environment for the investigation of different open-loop actuation strategies of an active fixture for chatter suppression, limiting the required actuation frequency within the actual bandwidth of the system.

The extensive numerical investigation carried out allowed highlighting the most influencing factors in assessing actuation effectiveness in suppressing the unstable vibrations. The results have shown that a pure sinusoidal actuation with frequency far from tooth-pass frequency and its harmonics is capable of disrupting the regenerative effect that generates the chatter instability. The achievable improvements have been formalized in terms of increased critical axial depth of cut, showing that the proposed actuation strategy could lead to evident improvement in achievable material removal rate in stable conditions, with the potential related benefits.

The results showed that the actuators embedded in the fixture should provide enough workpiece displacement at the actuation frequency to influence chip thickness. The achievable improvements in terms of achievable material removal rates are hence dependent on the displacement to feed per tooth ratio.

Developed actuation strategy could be an effective alternative to renowned closed-loop controls since it allows employing low-frequency actuation even for chatter frequencies that exceed the achievable actuation bandwidth, as in many practical applications. The fixture prototype is under assembly and further activities will be focused on testing the proposed actuation strategies on real cutting tests to experimentally validate the results.

### **Acknowledgements**

The authors would like to thank the DMG Mori Seiki Co. and the Machine Tool Technology Research Foundation (MTTRF) for the loaned machine tool (Mori Seiki NMV1500DCG 5-axes vertical-type machining center). This research was developed within the iNTEFIX project, founded from the European Community's Seventh Framework Program (FP7-2013-NMP-ICT-FoF) under grant agreement n. 609306.



## References

- Abele E, Hanselka H, Haase F, et al. (2008) Development and design of an active work piece holder driven by piezo actuators. *Production Engineering* 2(4): 437–442.
- Adriaens HJMT a., de Koning WL and Banning R (2000) Modeling piezoelectric actuators. *IEEE/ASME Transactions on Mechatronics* 5(4): 331–341.
- Altintas Y (2012) *Manufacturing Automation: Metal Cutting Mechanics, Machine Tool Vibrations, and CNC Design*. 2nd ed. Cambridge University Press.
- Altintas Y and Weck M (2004) Chatter Stability of Metal Cutting and Grinding. *CIRP Annals - Manufacturing Technology* 53(2): 619–642.
- Bathe KJ and Saunders H (1984) *Finite Element Procedures in Engineering Analysis*. *Journal of Pressure Vessel Technology*.
- Brecher C, Manoharan D, Ladra U, et al. (2010) Chatter suppression with an active workpiece holder. *Production Engineering* 4(2): 239–245.
- Ford DG, Myers a., Haase F, et al. (2013) Active Vibration Control for a CNC Milling Machine. *Proceedings of the Institution of Mechanical Engineers, Part C: Journal of Mechanical Engineering Science*.
- Ganguli a., Deraemaeker A, Romanescu I, et al. (2006) Simulation and Active Control of Chatter in Milling via a Mechatronic Simulator. *Journal of Vibration and Control* 12(8): 817–848.
- Grossi N, Sallese L, Scippa A, et al. (2015) Speed-varying cutting force coefficient identification in milling. *Precision Engineering* 42: 321–334.
- Grossi N, Scippa A, Sallese L, et al. (2015) Spindle speed ramp-up test: A novel experimental approach for chatter stability detection. *International Journal of Machine Tools and Manufacture* 89: 221–230.
- Hughes TJR (2000) *The finite element method: linear static and dynamic finite element analysis*. Dover Publications.
- Kyrychko YN and Hogan SJ (2010) On the Use of Delay Equations in Engineering Applications. *Journal of Vibration and Control* 16(7-8): 943–960.
- Montevocchi F, Grossi N, Scippa A, et al. (2016) Improved RCSA technique for efficient tool-tip dynamics prediction. *Precision Engineering*, doi:10.1016/j.precisioneng.2015.11.004
- Newmark NM (1959) A Method of Computation for Structural Dynamics. *Journal of the Engineering Mechanics Division* 85(7): 67–94.
- Park G, Bement MT, Hartman D a., et al. (2007) The use of active materials for machining processes: A review.

*International Journal of Machine Tools and Manufacture* 47(15): 2189–2206.

Quintana G and Ciurana J (2011) Chatter in machining processes: A review. *International Journal of Machine Tools and Manufacture* 51(5): 363–376.

Rashid A and Mihai Nicolescu C (2006) Active vibration control in palletised workholding system for milling. *International Journal of Machine Tools and Manufacture* 46(12-13): 1626–1636.

Scippa A, Sallese L, Grossi N, et al. (2015) Improved dynamic compensation for accurate cutting force measurements in milling applications. *Mechanical Systems and Signal Processing* 54-55: 314–324.

Weremczuk A, Rusinek R and Warminski J (2015) The Concept of Active Elimination of Vibrations in Milling Process. *Procedia CIRP* 31: 82–87.